

Robust Estimation of Effective Diffusions from Multiscale Data

Giacomo Garegnani ^{*} Andrea Zanoni ^{*}

Abstract

We present a methodology based on filtered data and moving averages for estimating robustly effective dynamics from observations of multiscale systems. We show in a semi-parametric framework of the Langevin type that the method we propose is asymptotically unbiased with respect to homogenization theory. Moreover, we demonstrate with a series of numerical experiments that the method we propose here outperforms traditional techniques for extracting coarse-grained dynamics from data, such as subsampling, in terms of bias and of robustness.

AMS subject classifications. 62F12, 65C30, 62M05.

Keywords. Parameter inference, diffusion processes, data-driven homogenization, filtering, moving average, Langevin equation.

1 Introduction

Inferring simple effective models from observations of complex phenomena characterized by multiple scales is a problem of interest in several fields, ranging from chemistry [16, 23], finance [6, 26], oceanography and meteorology [8, 15], and marine biology [15], among others. The issue of model misspecification due to the mismatch of complex multiscale data and simple models involving differential equations has been deeply studied, in particular for partial differential equations (PDEs) [1, 2, 4, 20] and for stochastic differential equations (SDEs) [3, 5, 9, 10, 13, 14, 22, 23].

In this paper, we are interested in inferring coarse-grained equations from observations of diffusion processes evolving on multiple time scales. Given a positive integer d , a drift function $b^\varepsilon: \mathbb{R}^d \times \mathbb{R}^d \rightarrow \mathbb{R}^d$ periodic with respect to its second argument, a multiscale parameter $\varepsilon > 0$, and a diffusion coefficient $\sigma > 0$, we consider the d -dimensional multiscale SDE

$$dX_t^\varepsilon = b^\varepsilon \left(X_t^\varepsilon, \frac{X_t^\varepsilon}{\varepsilon} \right) dt + \sqrt{2\sigma} dW_t, \quad (1.1)$$

where $W := (W_t, t \geq 0)$ is a standard d -dimensional Brownian motion, and where X_0^ε is a given initial condition. Assuming that data $X^\varepsilon := (X_t^\varepsilon, 0 \leq t \leq T)$ are provided, with T a finite final time, our goal is then inferring a coarse-grained equation, independent of the fastest scale $\mathcal{O}(\varepsilon^{-1})$, which reads

$$dX_t^0 = b^0(X_t^0) dt + \sqrt{2\Sigma} dW_t, \quad (1.2)$$

where $b^0: \mathbb{R}^d \rightarrow \mathbb{R}^d$ and $\Sigma \in \mathbb{R}^{d \times d}$ are the effective drift function and diffusion matrix, respectively. Knowledge of the full model (1.1) yields, in specific instances, a single-scale model (1.2) which is effective in the sense of the theory of homogenization. In particular, one can prove in these cases that $X^\varepsilon \rightarrow X^0$ for $\varepsilon \rightarrow 0$ in a weak sense. In this work, we consider b^ε and σ to be unknown and

^{*}ANMC, Institute of Mathematics, École Polytechnique Fédérale de Lausanne, 1015 Lausanne, Switzerland, giacomo.garegnani@epfl.ch, andrea.zanoni@epfl.ch

wish to infer the parameters of (1.2) from multiscale data. Hence, the problem we consider here could be framed into the setting of data-driven homogenization.

In this paper, we build on the techniques introduced in [3] and design a new class of estimators for effective diffusions based on filtered data. The methodologies we introduce here are easy to implement, computationally cheap, robust, and unbiased with respect to the theory of homogenization. In particular, the techniques studied in [3] are widened here to a vaster class of filters based on moving averages, which can be readily and simply employed for estimating effective diffusions. Furthermore, we complete the numerical analysis of [3] by testing our method against a complex instance of multi-dimensional Langevin equations.

1.1 Problem Setting

The class of multiscale SDEs which can be written as (1.1) is vast, and can be employed for modeling a wide range of physical and social phenomena. In this work, we narrow the scope by considering a semiparametric framework, and a gradient structure. In particular, given a positive integer N , known smooth functions $\{V_i: \mathbb{R}^d \rightarrow \mathbb{R}\}_{i=1}^N$ and an unknown function $p: \mathbb{R}^d \rightarrow \mathbb{R}$ periodic with period L_i in the i -th directions in \mathbb{R}^d for $i = 1, \dots, d$, we consider the drift

$$b^\varepsilon(x, y) = - \sum_{i=1}^N \alpha_i \nabla V_i(x) - \frac{1}{\varepsilon} \nabla p(y),$$

where $\{\alpha_i\}_{i=1}^N$ are unknown drift coefficients. In this way, equation (1.1) can be rewritten as

$$dX_t^\varepsilon = - \sum_{i=1}^N \alpha_i \nabla V_i(X_t^\varepsilon) dt - \frac{1}{\varepsilon} \nabla p\left(\frac{X_t^\varepsilon}{\varepsilon}\right) dt + \sqrt{2\sigma} dW_t, \quad (1.3)$$

so that the model we consider is of the overdamped Langevin type. For equation (1.3) there holds a homogenization result, which allows to compute, in case the drift and diffusion coefficients and the function p are known, an effective model such as (1.2). In particular, for any finite time horizon T , the solution of (1.3) $X^\varepsilon \rightarrow X^0$ weakly for $\varepsilon \rightarrow 0$ as random variables with values in $C^0([0, T]; \mathbb{R}^d)$, where $X^0 := (X_t^0, 0 \leq t \leq T)$ is the solution of

$$dX_t^0 = - \sum_{i=1}^N A_i \nabla V_i(X_t^0) dt + \sqrt{2\Sigma} dW_t. \quad (1.4)$$

Here, the matrices $A_i := \alpha_i \mathcal{K}$ and $\Sigma := \sigma \mathcal{K}$, where $\mathcal{K} \in \mathbb{R}^{d \times d}$ is the symmetric positive semidefinite matrix defined by

$$\mathcal{K} = \int_{\mathbb{L}} (I + D\Phi(y))(I + D\Phi(y))^\top d\mu(y), \quad \mathbb{L} := \bigotimes_{i=1}^d [0, L_i], \quad (1.5)$$

where $D\Phi$ is the Jacobian of the function $\Phi: \mathbb{R}^d \rightarrow \mathbb{R}^d$, solution of the vector-valued PDE, or cell problem

$$\begin{aligned} \mathcal{L}_0 \Phi &= \nabla p, & \text{in } \mathbb{L}, & \quad + \text{periodic b.c.}, \quad \text{on } \partial\mathbb{L}, \\ \int_{\mathbb{L}} \Phi(y) d\mu(y) &= 0, \end{aligned} \quad (1.6)$$

and where the differential operator \mathcal{L}_0 , applied component-wise to Φ , is defined as

$$\mathcal{L}_0 = -\nabla p \cdot \nabla + \sigma \Delta.$$

The measure μ introduced in (1.5) is the probability measure on \mathbb{L} given by

$$\mu(dy) = \frac{1}{C_\mu} \exp\left(-\frac{p(y)}{\sigma}\right) dy, \quad C_\mu = \int_{\mathbb{L}} \exp\left(-\frac{p(y)}{\sigma}\right) dy,$$

which accounts for the fluctuations at infinity of the fast-scales of the solution of (1.3).

In the statistical framework of data-driven homogenization, our goal is finding the matrices $\{A_i \in \mathbb{R}^{d \times d}\}_{i=1}^N$, and the matrix $\Sigma \in \mathbb{R}^{d \times d}$, given multiscale observations. In particular, since we assume that the function p , as well as the drift and diffusion coefficients appearing in (1.3), are unknown, the statistical approach is the only viable option for determining an effective equation. Our goal is then designing a methodology to determine the $N \times d \times d$ coefficients and the $d \times d$ coefficients defining the effective drift and diffusion, respectively, consistently with the theory of homogenization, so that the inferred model is indeed a coarse-grained surrogate describing the multiscale data.

1.2 Outline

The remainder of this paper is organized as follows. In Section 2 we present our methodology and introduce the main results of unbiasedness for the estimators based on filtered data. We then present numerical experiments in Section 3 corroborating our theoretical findings and showing how to apply our methodology to a complex multi-dimensional scenario. Section 4 is dedicated to the proof of unbiasedness for our estimators, which is achieved employing techniques that we inherit from our previous work [3]. We finally draw our conclusions in Section 5.

2 The Filtered Data Approach

It is known (see e.g. [23]) that some form of preprocessing is needed when one wishes to fit effective diffusion processes to multiscale data. In [23], and other related works, preprocessing is achieved by subsampling the data at an appropriate rate, which lies between the characteristic time scales of the multiscale and the homogenized processes. As we observed in our previous work [3], effective diffusions inferred with subsampling are strongly dependent on the subsampling rate. Therefore, we propose instead to preprocess the data by filtering them with a low-pass linear time-invariant filter. In particular, we consider in [3] an exponential filtering kernel of the form

$$k_{\text{exp}}^{\delta, \beta}(r) = \frac{C_\beta}{\delta^{1/\beta}} \exp\left(-\frac{r^\beta}{\delta}\right), \quad C_\beta = \frac{\beta}{\Gamma(1/\beta)}, \quad (2.1)$$

where the constant C_β normalizes the kernel in the sense

$$\int_0^\infty k_{\text{exp}}^{\delta, \beta}(r) dr = 1.$$

We notice that the parameters δ and β in (2.1) have two different roles. In particular, we have that β is a *shape parameter*, and δ is the *filtering width*. Given the kernel $k_{\text{exp}}^{\delta, \beta}$, a preprocessed filtered trajectory is computed by taking a time convolution as

$$Z_t^\varepsilon = \int_0^t k_{\text{exp}}^{\delta, \beta}(t-s) X_s^\varepsilon ds.$$

It is demonstrated, always in [3], that the results of an appropriate estimating procedure based on the filtered data are more robust than subsampling, especially if (2.1) is employed with the coefficient $\beta > 1$. We prove theoretically in [3], though, asymptotic unbiasedness of our estimation procedure only when $\beta = 1$, which appears to be the least robust choice for the shape parameter. Moreover, it can be observed that the estimators computed with data filtered employing the kernel $k_{\text{exp}}^{\delta, \beta}$ stabilize fast with respect to growing values of β , independently of the filtering width δ . It appears then natural to take the limit $\beta \rightarrow \infty$, and to study the limiting filtering kernel. In particular, it is simple to deduce that for almost every $r \geq 0$

$$\lim_{\beta \rightarrow \infty} k_{\text{exp}}^{\delta, \beta}(r) = \chi_{[0,1]}(r), \quad (2.2)$$

independently of δ , where $\chi_{[a,b]}$ denotes the indicator function of the interval $[a, b]$ for real numbers $a < b$. Taking the convolution of the data with the limiting kernel given in (2.2), we obtain the filtered trajectory

$$Z_t^\varepsilon = \int_{t-1}^t X_s^\varepsilon ds.$$

Reintroducing a parameter $\delta > 0$ of filtering width into the limiting kernel yields the family of *moving average* kernels

$$k_{\text{ma}}^\delta(r) = \frac{1}{\delta} \chi_{[0,\delta]}(r),$$

which, applied to the data, give the filtered trajectory defined as

$$Z_t^\varepsilon = \frac{1}{\delta} \int_{t-\delta}^t X_s^\varepsilon ds.$$

Summarizing, the relationships between the filtering kernel presented in [3] and the one considered here are given by the following scheme:

$$k_{\text{exp}}^{\delta,\beta} \xrightarrow{\beta \rightarrow \infty, \forall \delta > 0} k_{\text{ma}}^1 \xleftarrow{\delta \rightarrow 1} k_{\text{ma}}^\delta.$$

The application of a moving average to multiscale data and the estimation of effective diffusions based on this preprocessing techniques are then the main topic of this paper.

We now present how in practice one employs filtered data for estimating effective diffusion models of the form (1.4), coherently with the theory of homogenization, and given multiscale data. Let us consider from now on for clarifying the discussion the case $d = 1$, for which equation (1.3) reads

$$dX_t^\varepsilon = - \sum_{i=1}^N \alpha_i V_i'(X_t^\varepsilon) dt - \frac{1}{\varepsilon} p' \left(\frac{X_t^\varepsilon}{\varepsilon} \right) dt + \sqrt{2\sigma} dW_t.$$

We introduce the compact notation $V: \mathbb{R} \rightarrow \mathbb{R}^N$, $V: x \mapsto (V_1(x), V_2(x), \dots, V_N(x))^\top$, and write $V'(x)$ for the component-wise derivative of the vector-valued function V . Likewise [3], we then modify the classical maximum likelihood estimator based on Girsanov formula (see e.g. [17, 18, 21, 25]), and define a new estimator $\widehat{A}(X^\varepsilon, T)$ for the effective drift coefficient as the solution of the linear system

$$\begin{aligned} -M(X^\varepsilon) \widehat{A}(X^\varepsilon, T) &= v(X^\varepsilon), \\ M(X^\varepsilon) &:= \frac{1}{T} \int_0^T V'(Z_t^\varepsilon) \otimes V'(X_t^\varepsilon) dt, \quad v(X^\varepsilon) := \frac{1}{T} \int_0^T V'(Z_t^\varepsilon) dX_t^\varepsilon. \end{aligned} \quad (2.3)$$

We remark that it is fundamental to keep X_t^ε in the differential of the right-hand side $v(X^\varepsilon)$, as widely discussed in [3]. Coherently with [3], we define the estimator of the effective diffusion coefficient as

$$\widehat{\Sigma}(X^\varepsilon, T) = \frac{1}{\delta T} \int_\delta^T (X_t^\varepsilon - Z_t^\varepsilon) (X_t^\varepsilon - X_{t-\delta}^\varepsilon) dt.$$

Once the homogenized drift and diffusion coefficients are estimated, we have in the semi-parametric framework a full definition of the effective equation.

Remark 2.1. In order to treat initial conditions, which are negligible in the limit of large data, we define for $t < \delta$ the filtered trajectory as

$$Z_t^\varepsilon = \frac{1}{t} \int_0^t X_s^\varepsilon ds, \quad 0 \leq t < \delta.$$

Remark 2.2. The choice $d = 1$ is made here only for economy of notation, and for enhancing the clarity of our exposition. Indeed, as we will present in numerical experiments, our methodology based on filtered data can be successfully applied to higher-dimensional SDEs. Moreover, proving asymptotic unbiasedness would not entail additional difficulties in case $d > 1$, but the clarity of the proof of our theoretical results is enhanced by the choice of treating the one-dimensional case.

We report here the expression of the estimators for higher dimensions. Let $\nabla V: \mathbb{R}^d \rightarrow \mathbb{R}^{dN}$ be the vector obtained by stacking the gradients of the components V_i , $i = 1, \dots, N$ of the slow-scale potential, i.e.,

$$\nabla V(x) = (\nabla V_1(x)^\top \quad \dots \quad \nabla V_N(x)^\top)^\top.$$

Then, the drift estimator for the block matrix $A \in \mathbb{R}^{dN \times d}$ given by

$$A = (A_1^\top \quad \dots \quad A_N^\top)^\top,$$

is the solution of the linear system

$$-M(X^\varepsilon) \widehat{A}(X^\varepsilon, T) = v(X^\varepsilon),$$

where the matrices $M(X^\varepsilon) \in \mathbb{R}^{dN \times dN}$ and $v(X^\varepsilon) \in \mathbb{R}^{dN \times d}$ are defined as

$$M(X^\varepsilon) := \frac{1}{T} \int_0^T \nabla V(Z_t^\varepsilon) \otimes \nabla V(X_t^\varepsilon) dt, \quad v(X^\varepsilon) := \frac{1}{T} \int_0^T \nabla V(Z_t^\varepsilon) \otimes dX_t^\varepsilon.$$

Moreover, the estimator for the effective diffusion coefficients in dimension d reads

$$\widehat{\Sigma}(X^\varepsilon, T) = \frac{1}{\delta T} \int_0^T (X_t^\varepsilon - Z_t^\varepsilon) \otimes (X_t^\varepsilon - X_{t-\delta}^\varepsilon) dt \in \mathbb{R}^{d \times d}.$$

2.1 Statement of the Main Results

We first introduce the assumptions which will be employed in the theoretical analysis. In particular, we place ourselves in the same dissipative framework as in [3, 23].

Assumption 2.3. The potentials p and V satisfy

- (i) the function $p \in \mathcal{C}^\infty(\mathbb{R})$ is L -periodic for some $L > 0$;
- (ii) the functions $V_i \in \mathcal{C}^\infty(\mathbb{R})$ for all $i = 1, \dots, N$ are polynomially bounded from above and bounded from below. Moreover, the potential is dissipative, i.e., there exist $a, b > 0$ such that

$$-\alpha \cdot V'(x)x \leq a - bx^2;$$

- (iii) the functions V' and V'' are Lipschitz continuous, i.e., there exists a constant $C > 0$ such that

$$\|V'(x) - V'(y)\| \leq C|x - y|, \quad \text{and} \quad \|V''(x) - V''(y)\| \leq C|x - y|,$$

where $\|\cdot\|$ denotes the Euclidean norm, and the components V'_i and V''_i are polynomially bounded for all $i = 1, \dots, N$;

- (iv) for all $T > 0$, the matrix $M(X^\varepsilon)$ defined in (2.3) is invertible.

Our main theoretical findings are then summarized by the two following theorems, which state that our estimators are asymptotically unbiased for the effective coefficients, and thus allow to retrieve correct coarse-grained models from multiscale data.

Theorem 2.4. *Under Assumption 2.3, it holds if δ is independent of ε*

$$\lim_{\varepsilon \rightarrow 0} \lim_{T \rightarrow \infty} \widehat{A}(X^\varepsilon, T) = A, \quad a.s., \quad (2.4)$$

and if $\delta = \varepsilon^\zeta$ with $\zeta \in (0, 2)$

$$\lim_{\varepsilon \rightarrow 0} \lim_{T \rightarrow \infty} \widehat{A}(X^\varepsilon, T) = A, \quad a.s. \quad (2.5)$$

Theorem 2.5. *Under Assumption 2.3, it holds if $\delta = \varepsilon^\zeta$ with $\zeta \in (0, 2)$,*

$$\lim_{\varepsilon \rightarrow 0} \lim_{T \rightarrow \infty} \widehat{\Sigma}(X^\varepsilon, T) = \Sigma, \quad a.s.$$

The proof of Theorems 2.4 and 2.5 is obtained by applying techniques similar to the ones employed in [3, 5], and is presented in detail in Section 4.

$A = 0.624$	β				k_{ma}^1
δ	1	2	5	10	–
1	0.644	0.634	0.633	0.634	0.635
$\varepsilon^{1/2}$	0.637	0.631	0.630	0.632	0.635
ε	0.662	0.636	0.628	0.629	0.635
$\varepsilon^{3/2}$	0.726	0.650	0.628	0.627	0.635
ε^2	0.837	0.671	0.631	0.627	0.635

Table 1: Estimator of the effective drift coefficient obtained with $k_{\text{exp}}^{\delta,\beta}$ for several values of δ and β , compared with k_{ma}^1 . On the top left corner, the true value of the homogenized drift coefficient.

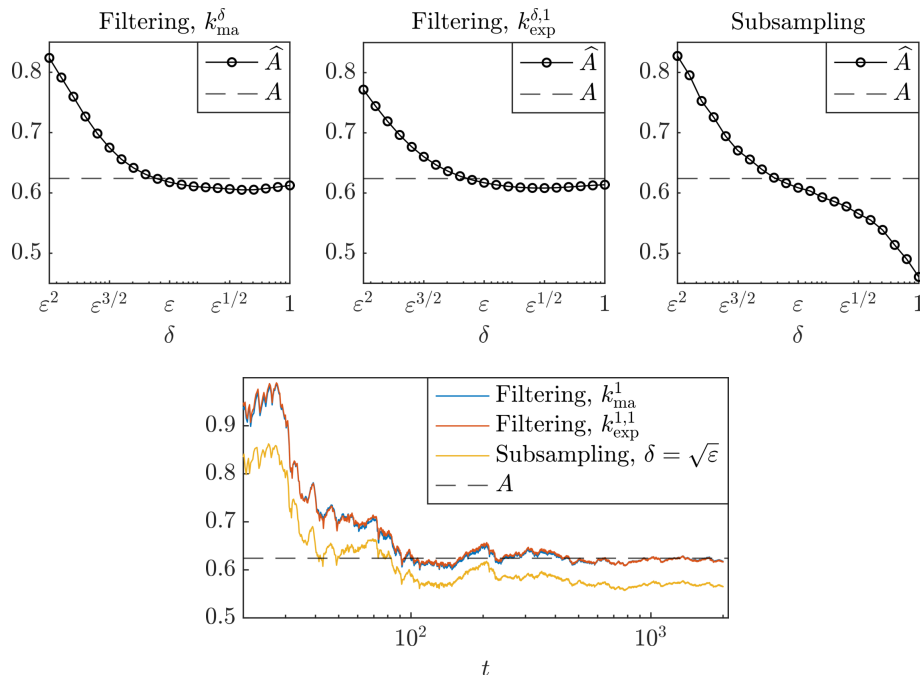


Figure 1: Sensitivity analysis for the estimation of the drift coefficient. Top: Sensitivity with respect to the filtering width δ of the drift estimator given by the filtering kernels k_{ma}^{δ} and $k_{\text{exp}}^{\delta,\beta}$, as well as of subsampling. Bottom: Time evolution of the estimators for $t \in [0, 2000]$.

3 Numerical Experiments

In this section, we present a series of numerical experiments which have the twofold goal of validating our theoretical analysis, and of showcasing the effectiveness of our technique on challenging academic examples.

3.1 Sensitivity Analysis with a Ornstein–Uhlenbeck Model

We first perform a sensitivity analysis of the filtering approach based on moving averages, and a comparison with the exponential filter and with subsampling. For this purpose, we employ a simple multiscale Ornstein–Uhlenbeck model. In particular, we consider equation (1.3) with $d = N = 1$, with the slow scale potential $V(x) = x^2/2$, and with the fluctuating potential $p(y) = \cos(y)$. Moreover, we fix the drift coefficient in the multiscale model to $\alpha = 1$, the diffusion coefficient $\sigma = 1$, and the multiscale parameter $\varepsilon = 0.05$. We then generate synthetic data $X^\varepsilon = (X_t^\varepsilon, 0 \leq t \leq 2000)$ with the Euler–Maruyama method computed with a fine time step (negligible with respect to ε^2).

As a first experiment, we demonstrate how $k_{\text{exp}}^{\delta,\beta} \rightarrow k_{\text{ma}}^1$, together with the associated estimators of

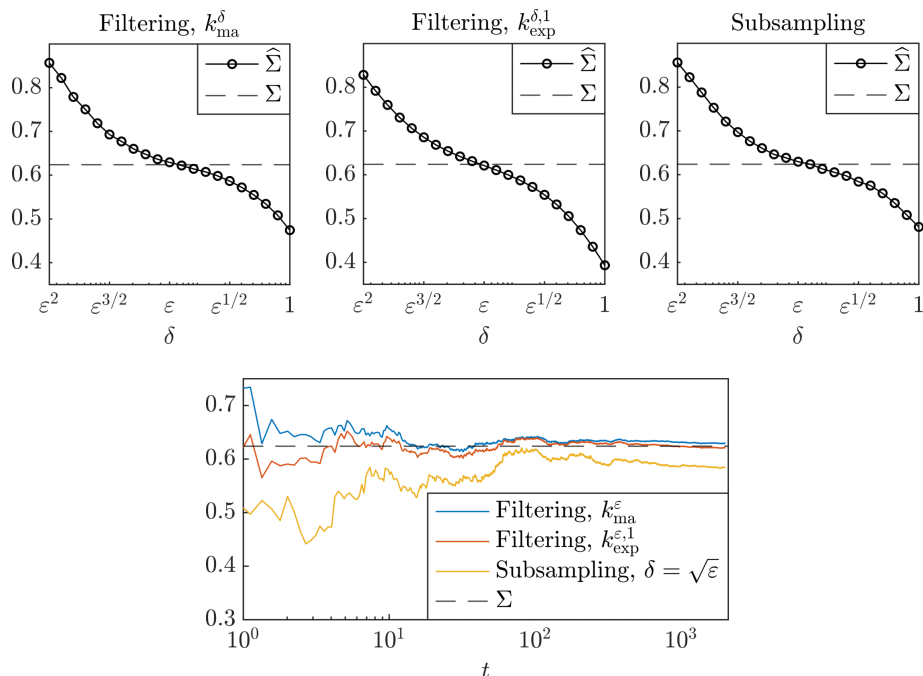
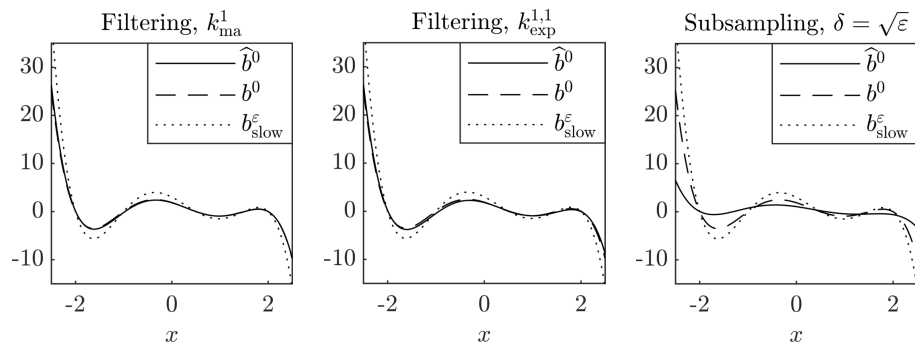


Figure 2: Sensitivity analysis for the estimation of the diffusion coefficient. Top: Sensitivity with respect to the filtering width δ of the diffusion estimator given by the filtering kernels k_{ma}^δ and $k_{\text{exp}}^{\delta,1}$, as well as of subsampling. Bottom: Time evolution of the estimators for $t \in [0, 2000]$.

the drift coefficient, for $\beta \rightarrow \infty$ and independently of δ . Results are presented in Table 1, where it is confirmed empirically that the estimator stabilizes with respect to the filtering width δ when the shape parameter β is chosen larger.

In the second experiment, we verify the dependence on the filtering width δ of the moving average filter k_{ma}^δ and comparing with the dependence on δ of $k_{\text{exp}}^{\delta,1}$. Results, given in Fig. 1, show that the filter k_{ma}^δ yields good results, in this instance, for all values of $\delta \in [\varepsilon, 1]$. The theoretical result of Theorem 2.4, predicting that all values in $\delta \in (\varepsilon^2, 1]$ yield unbiased estimators, is respected, but asymptotically. Comparing with $k_{\text{exp}}^{\delta,1}$, we notice that results are extremely similar. As a matter of comparison, we show always in Fig. 1 that instead subsampling does not seem a viable option for robustly inferring the effective drift coefficient. For the optimal implementation of k_{ma}^δ and $k_{\text{exp}}^{\delta,1}$, which appears to be with $\delta = 1$, we give always in Fig. 1 the time evolution of the drift estimator for $t \in [0, 2000]$. For completeness, we compare the time evolution of the drift estimator given by subsampling implemented with $\delta = \sqrt{\varepsilon}$, which lays in the middle of the theoretical validity for the subsampling width [23]. We notice that the choice $T = 2000$ for our sensitivity analysis is fully justified, as the estimators seem to stabilize with respect to time at around $t = 10^3$.

In the third and last experiment, we consider the estimation of the effective diffusion coefficient. As above, we compare the estimators based on filtered data and obtained with k_{ma}^δ , $k_{\text{exp}}^{\delta,1}$, and with subsampling. For the definition of the estimators obtained with the two latter methods, we refer to [3] and [23], respectively. In Fig. 2, we show the dependence of the estimators on the parameter δ , which we vary in the interval $\delta \in [\varepsilon^2, 1]$. We notice that all the three estimators have a similar rather strong dependence on the filtering (or subsampling) width δ . In particular, in all cases the choice $\delta = \varepsilon$ seems to yield optimal results. As for the drift coefficient, we verify numerically that results stabilize with respect to time at around $t = 10^3$, so that our choice of the final time for the sensitivity analysis with respect to δ is justified. For completeness, we compare the time evolution of the diffusion estimator given by subsampling implemented with $\delta = \sqrt{\varepsilon}$, which lays in the middle of the theoretical validity for the subsampling width [23].



Parameter	Truth	Filtering, k_{ma}^1	Filtering, $k_{\text{exp}}^{1,1}$	Subsampling, $\delta = \sqrt{\varepsilon}$
A_1	0.62	0.63	0.60	0.18
A_2	-0.62	-0.66	-0.69	-0.19
A_3	-3.28	-3.24	-3.07	-1.04
A_4	2.96	3.07	3.20	1.09
A_5	3.12	2.98	2.71	1.45
A_6	-1.87	-1.84	-1.81	-1.06
Relative Error		0.03	0.09	0.61

Figure 3: Numerical results for the experiment of Section 3.2. Top: Visual comparison of the estimated effective drift functions \hat{b}^0 , obtained with filtering kernels k_{ma}^1 , $k_{\text{exp}}^{1,1}$, and subsampling. Bottom: Numerical values of the estimated effective drift coefficients.

3.2 Effective Drift Function for One-dimensional Diffusions

We now consider a one-dimensional multiscale Langevin equation and a six-dimensional drift coefficient defining the slow-scale potential. With a reference to the notation introduced in (1.3), we choose $V_i = x^i/i$ for $i = 1, \dots, 6$, the fast-scale potential $p = \cos(y)$, the diffusion coefficient $\sigma = 1$ and the multiscale parameter $\varepsilon = 0.05$. The true drift coefficients in the multiscale equations are chosen as $\alpha_1 = 1$, $\alpha_2 = -2$, $\alpha_3 = -5.25$, $\alpha_4 = 4.75$, $\alpha_5 = 5$, and $\alpha_6 = -3$. We then generate synthetic data $X^\varepsilon := (X_t, 0 \leq t \leq 2000)$ with the Euler–Maruyama method computed with a fine time step, and wish to infer from data the effective drift coefficients A_i , $i = 1, \dots, 6$. For this purpose, we compare the moving average introduced here and implemented with $\delta = 1$, i.e., the kernel k_{ma}^1 , with the optimal choice of the filtering methodology introduced in [3] corresponding to the kernel $k_{\text{exp}}^{1,1}$, and with subsampling. For the latter, we choose a subsampling width of $\delta = \sqrt{\varepsilon}$. Numerical results, shown in Fig. 3, demonstrate that the approach based on moving averages outperforms both exponential filtering and subsampling. We measure accuracy in terms of relative error, which is measured as

$$\text{Relative Error} = \frac{\|A - \hat{A}\|}{\|A\|},$$

where \hat{A} is alternatively the six-dimensional drift coefficient estimated with one of the three techniques.

3.3 Effective Drift Function for Two-dimensional Diffusions

We now consider a two-dimensional SDE (i.e., $d = 2$) of the form (1.3). In particular, we choose a slow-scale potential with $N = 4$ components defined as

$$\begin{aligned} V_1(x) &= \exp\left(-\|x - x_1\|^2\right), & V_2(x) &= \exp\left(-\|x - x_2\|^2\right), \\ V_3(x) &= \exp\left(-\|x\|^2\right), & V_4(x) &= \frac{1}{4}\|x\|^4, \end{aligned}$$

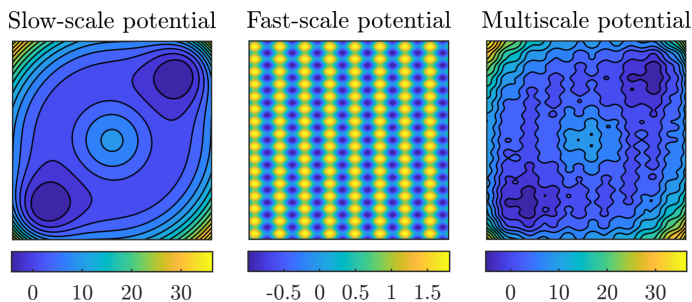


Figure 4: Slow, fast, and multiscale potentials for the two-dimensional experiment of Section 3.3. The functions are depicted here on the square $(-2.5, 2.5)^2$.

where $x_1 = (2, 2)^\top$, $x_2 = (-2, -2)^\top$, and pre-multiplied by the drift coefficients $\alpha_1 = \alpha_2 = -15$, $\alpha_3 = 10$ and $\alpha_4 = 1$, respectively. We then define a fast-scale periodic potential $p: \mathbb{R}^2 \rightarrow \mathbb{R}$ as

$$p(y) = \sin(y_1) + \sin^2(y_2).$$

The slow, fast, and multiscale potential functions are represented in Fig. 4. We note that the slow-scale potential presents two local minima due to the Gaussian functions V_1 and V_2 , which are multiplied by negative scalars, a local maximum in the origin due to the Gaussian component V_3 , and escapes to infinity due to the quartic potential V_4 , which dominates the other terms outside any ball large enough and centered in the origin. As shown in Fig. 4, the superposition of the slow and fast-scale potentials (evaluated in $y = x/\varepsilon$) perturbs the slow-scale potential and is responsible for an infinity of non-negligible local minima.

We generate synthetic observations $X^\varepsilon = (X_t^\varepsilon, 0 \leq t \leq T)$ by integrating with Euler–Maruyama with a small time step (negligible with respect to ε^2) the dynamics (1.3), which we remind being defined as

$$dX_t^\varepsilon = - \sum_{i=1}^4 \alpha_i \nabla V_i(X_t^\varepsilon) - \frac{1}{\varepsilon} \nabla p\left(\frac{X_t^\varepsilon}{\varepsilon}\right) + \sqrt{2\sigma} dW_t,$$

where we fix the diffusion coefficient $\sigma = 1.25$ and the multi scale parameter $\varepsilon = 0.1$. With these choices, the homogenization matrix \mathcal{K} defined in (1.5) is diagonal, and approximately reads

$$\mathcal{K} = \begin{pmatrix} 0.74 & 0 \\ 0 & 0.92 \end{pmatrix},$$

which fully defines the effective dynamics driven by equation (1.4). Our goal is then estimating the effective drift coefficients $\{A_i \in \mathbb{R}^{2 \times 2}\}_{i=1}^4$ from observations. For this purpose, we employ

- (i) Data filtered with the kernel $k_{\text{ma}}^1(r) = \chi_{[0,1]}(r)$, and the corresponding estimator $\widehat{A}(X^\varepsilon, T)$;
- (ii) Data filtered with the kernel $k_{\text{exp}}^{1,1}(r) = \exp(-r)$, i.e., the filter (2.1) explored in [3], implemented with $\delta = \beta = 1$, and the corresponding estimator $\widehat{A}(X^\varepsilon, T)$;
- (iii) Subsampled data, with subsampling frequency $\delta = \sqrt{\varepsilon}$, and its corresponding estimator.

We test all the three strategies above for final times $T = \{500, 1000, 2000\}$, in order to notice the time evolution of the estimators. Numerical results are given in Fig. 5, Fig. 6 and Fig. 7 for all the strategies above, respectively. In particular, since the homogenized drift cannot be expressed as the gradient of a potential function, we represent the two components of the function b^0 defined as

$$b^0(x) = - \sum_{i=1}^4 A_i \nabla V_i(x),$$

coherently with the notation introduced in (1.2), where $\{A_i\}_{i=1}^4$ are in turn replaced by the estimators given by the three strategies above. Heuristically, we remark that the estimator given by

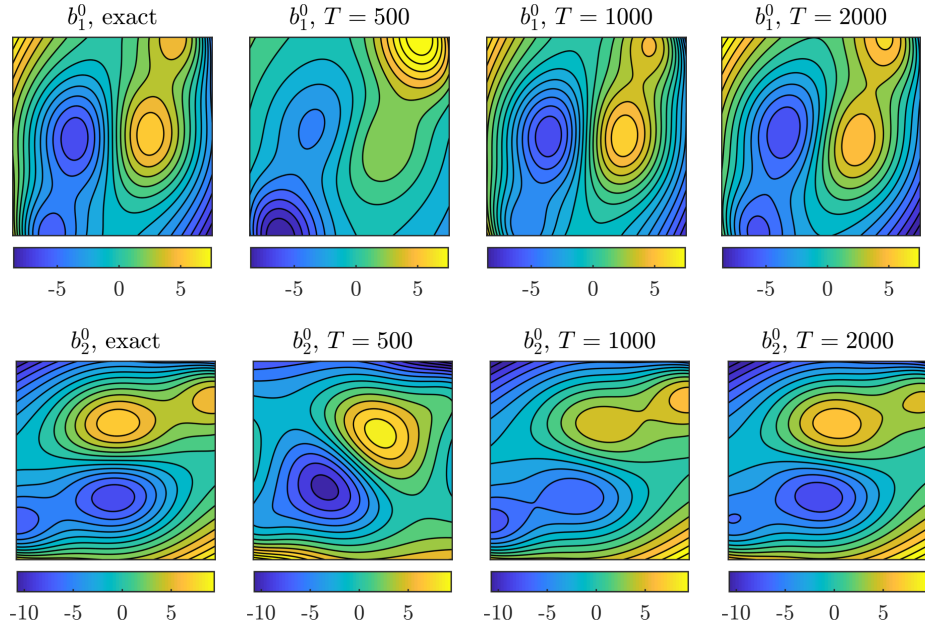


Figure 5: Numerical results for the moving average filter k_{ma}^1 for the two-dimensional experiment of Section 3.3. The inferred drift function (first and second component, per row) are depicted here on the square $(-2.5, 2.5)^2$. On the first column, we give the exact drift function. On the second to fourth column, the estimation results for $T = 500, 1000, 2000$ respectively.

strategy (i) above, i.e., the new technique we introduce in this paper, estimates better the effective drift function than the strategies (ii), and especially (iii). The improvement over the two previously existing techniques is made more evident in Table 2, where numerical results for the 16 estimated coefficients are presented together for the three estimation strategies. In particular, we measure in the last row of Table 2 the relative error as

$$\text{Relative error} = \frac{\|\mathbf{A} - \hat{\mathbf{A}}\|}{\|\mathbf{A}\|},$$

where $\|\cdot\|$ is the Euclidean norm, where $\mathbf{A} \in \mathbb{R}^{16}$ is the vector of all coefficients appearing in the matrices A_i , $i = 1, \dots, 4$, with standard ordering, and where $\hat{\mathbf{A}}$ is the corresponding vector of estimated coefficients, with all three strategies (i)–(iii).

4 Asymptotic Unbiasedness

In this section we present the proof of Theorems 2.4 and 2.5, the results of asymptotic unbiasedness for our filtering-based estimators. In [3], proofs of convergence are obtained with the kernel $k_{\text{exp}}^{\delta, 1}$, by noticing that in this case the original trajectory X^ε and its filtered version Z^ε are solution of the hypoelliptic system of Itô SDEs

$$\begin{aligned} dX_t^\varepsilon &= -\alpha \cdot V'(X_t^\varepsilon) dt - \frac{1}{\varepsilon} p' \left(\frac{X_t^\varepsilon}{\varepsilon} \right) dt + \sqrt{2\sigma} dW_t, \\ dZ_t^\varepsilon &= -\frac{1}{\delta} (Z_t^\varepsilon - X_t^\varepsilon) dt. \end{aligned}$$

For higher values of $\beta > 1$, the system describing the evolution of X_t^ε and Z_t^ε is not a Itô system due to the presence of a memory term. In case we take the limit $\beta \rightarrow \infty$, and reintroduce the filtering width δ to obtain the kernel k_{ma}^δ we study in this paper, the memory term simplifies to a constant delay, and the evolution of the filtered trajectory Z_t^ε can be coupled with the original

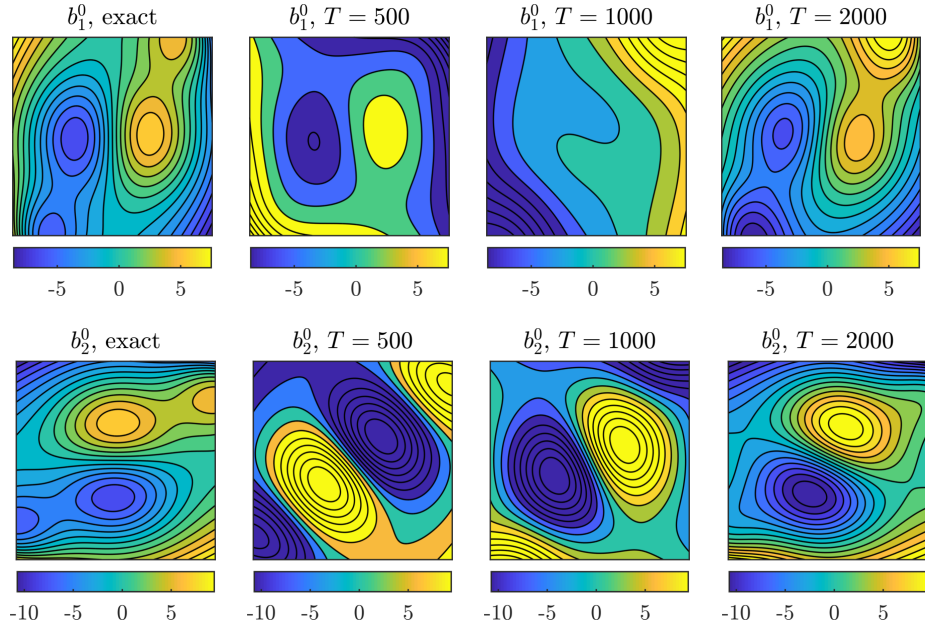


Figure 6: Numerical results for the exponential filter $k_{\text{exp}}^{1,1}$ for the two-dimensional experiment of Section 3.3. The inferred drift function (first and second component, per row) are depicted here on the square $(-2.5, 2.5)^2$. On the first column, we give the exact drift function. On the second to fourth column, the estimation results for $T = 500, 1000, 2000$ respectively.

trajectory X_t^ε through the system of stochastic delay differential equations (SDDEs)

$$\begin{aligned} dX_t^\varepsilon &= -\alpha \cdot V'(X_t^\varepsilon) dt - \frac{1}{\varepsilon} p' \left(\frac{X_t^\varepsilon}{\varepsilon} \right) dt + \sqrt{2\sigma} dW_t, \\ dZ_t^\varepsilon &= -\frac{1}{\delta} (X_{t-\delta}^\varepsilon - X_t^\varepsilon) dt. \end{aligned} \quad (4.1)$$

To be precise, the system above is not entirely a system of SDDEs, but it is a combination of a Itô SDE, and a delay ordinary differential equation driven by a stochastic signal. Due to the theory of homogenization (see [7, Chapter 3], or [24, Chapter 18], or the proof of [3, Lemma 3.9]), if δ is independent of ε , the solution $(X^\varepsilon, Z^\varepsilon)$ converges in law as random variable in $C^0([0, T], \mathbb{R}^2)$ to the solution (X^0, Z^0) of the system

$$\begin{aligned} dX_t^0 &= -A \cdot V'(X_t^0) dt + \sqrt{2\Sigma} dW_t, \\ dZ_t^0 &= -\frac{1}{\delta} (X_{t-\delta}^0 - X_t^0) dt. \end{aligned} \quad (4.2)$$

In the following, we first focus on ergodic properties of the couples $(X^\varepsilon, Z^\varepsilon)$ and (X^0, Z^0) evolving according to (4.1) and (4.2), respectively. Then, we employ the invariant measures and the Fokker-Planck equations derived through ergodicity theory to prove asymptotic unbiasedness. Let us remark that the strategy of our proof is similar to the one of [3]. Still, different techniques need to be employed due to the delay in the second equation of the systems (4.1) and (4.2).

4.1 Ergodic Properties

It is well-known (see e.g. [3, 23]) that X^ε is geometrically ergodic with invariant measure μ^ε on \mathbb{R} , whose density ρ^ε satisfying $\mu^\varepsilon(dx) = \rho^\varepsilon(x) dx$ takes the Gibbs form

$$\rho^\varepsilon(x) = \frac{1}{C_x^\varepsilon} \exp \left(-\frac{V_\varepsilon(x)}{\sigma} \right), \quad C_x^\varepsilon = \int_{\mathbb{R}} \exp \left(-\frac{V_\varepsilon(x)}{\sigma} \right) dx,$$

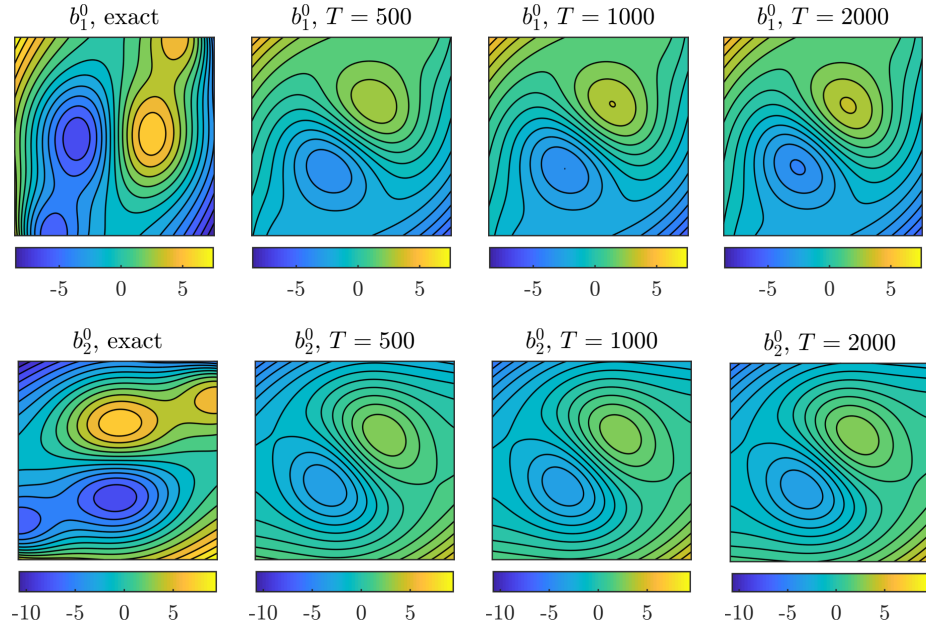


Figure 7: Numerical results for subsampling, with $\delta = \sqrt{\varepsilon}$ for the two-dimensional experiment of Section 3.3. The inferred drift function (first and second component, per row) are depicted here on the square $(-2.5, 2.5)^2$. On the first column, we give the exact drift function. On the second to fourth column, the estimation results for $T = 500, 1000, 2000$ respectively.

where

$$V_\varepsilon(x) := \alpha \cdot V(x) + p\left(\frac{x}{\varepsilon}\right).$$

Moreover, an analogous result holds true for the homogenized process X^0 , which is geometrically ergodic with invariant measure μ^0 on \mathbb{R} , whose density ρ^0 satisfying $\mu^0(dx) = \rho^0(x) dx$ is given by

$$\rho^0(x) = \frac{1}{C_x^0} \exp\left(-\frac{A \cdot V(x)}{\Sigma}\right), \quad C_x^0 = \int_{\mathbb{R}} \exp\left(-\frac{A \cdot V(x)}{\Sigma}\right) dx.$$

We now introduce a similar result of ergodicity for the couples $(X^\varepsilon, Z^\varepsilon)$ and (X^0, Z^0) satisfying (4.1) and (4.2), respectively, i.e., for the multiscale process and its filtered version.

Proposition 4.1. *The solution $(X^\varepsilon, Z^\varepsilon)$ of (4.1) is ergodic, and the density $\tilde{\rho}^\varepsilon$ of its invariant measure $\tilde{\mu}^\varepsilon$ on \mathbb{R}^2 , such that $\tilde{\mu}^\varepsilon(dx, dz) = \tilde{\rho}^\varepsilon(x, z) dx dz$, satisfies*

$$\begin{aligned} \sigma \partial_{xx}^2 \tilde{\rho}^\varepsilon(x, z) + \partial_x (V'_\varepsilon(x) \tilde{\rho}^\varepsilon(x, z)) + \frac{1}{\delta} \partial_z \left(\left(\int_{\mathbb{R}} y \psi^\varepsilon(y | x, z) dy - x \right) \tilde{\rho}^\varepsilon(x, z) \right) &= 0, \\ \int_{\mathbb{R}} \int_{\mathbb{R}} \tilde{\rho}^\varepsilon(x, z) dx dz &= 1, \end{aligned} \quad (4.3)$$

where, if $X_0^\varepsilon \sim \mu^\varepsilon$, it holds

$$\int_{\mathbb{R}} y \psi^\varepsilon(y | x, z) dy = \mathbb{E}[X_0^\varepsilon | X_\delta^\varepsilon = x, Z_\delta^\varepsilon = z],$$

i.e., $\psi^\varepsilon(\cdot | x, z)$ is the conditional density of X_0^ε given $X_\delta^\varepsilon = x$ and $Z_\delta^\varepsilon = z$. Moreover, if δ is independent of ε , the solution (X^0, Z^0) of (4.2) is ergodic, and the density $\tilde{\rho}^0$ of its invariant measure $\tilde{\mu}^0$ on \mathbb{R}^2 , such that $\tilde{\mu}^0(dx, dz) = \tilde{\rho}^0(x, z) dx dz$, satisfies

$$\begin{aligned} \Sigma \partial_{xx}^2 \tilde{\rho}^0(x, z) + \partial_x (A \cdot V'(x) \tilde{\rho}^0(x, z)) + \frac{1}{\delta} \partial_z \left(\left(\int_{\mathbb{R}} y \psi^0(y | x, z) dy - x \right) \tilde{\rho}^0(x, z) \right) &= 0, \\ \int_{\mathbb{R}} \int_{\mathbb{R}} \tilde{\rho}^0(x, z) dx dz &= 1, \end{aligned} \quad (4.4)$$

Parameter	Truth	Filtering, k_{ma}^1			Filtering, $k_{\text{exp}}^{1,1}$			Subsampling, $\delta = \sqrt{\varepsilon}$		
		$T(\cdot 10^3)$			$T(\cdot 10^3)$			$T(\cdot 10^3)$		
		0.5	1	2	0.5	1	2	0.5	1	2
$(A_1)_{11}$	-11.02	-13.82	-10.50	-11.25	-19.78	-10.40	-11.23	-1.33	-1.25	-1.23
$(A_1)_{12}$	0	-3.08	-1.85	-1.69	-12.08	-1.08	-1.40	-0.44	-0.48	-0.44
$(A_1)_{21}$	0	2.76	-0.24	-0.44	-20.18	13.80	1.86	-0.11	-0.16	-0.16
$(A_1)_{22}$	-13.86	-14.00	-14.96	-13.63	-34.98	-11.17	-11.95	-0.69	-0.68	-0.71
$(A_2)_{11}$	-11.02	-12.22	-8.96	-9.82	-16.97	-10.12	-10.00	-1.11	-0.96	-0.92
$(A_2)_{12}$	0	-1.62	-1.66	-2.01	-9.19	-1.09	-1.64	-0.50	-0.46	-0.42
$(A_2)_{21}$	0	3.02	-0.09	-0.09	-19.67	14.58	2.34	-0.05	-0.12	-0.14
$(A_2)_{22}$	-13.86	-14.99	-14.79	-13.09	-35.78	-11.02	-11.56	-0.62	-0.67	-0.69
$(A_3)_{11}$	7.35	3.63	7.44	7.18	14.57	-0.29	6.69	2.18	2.42	2.65
$(A_3)_{12}$	0	-1.10	-0.36	-1.24	1.77	-0.71	-0.97	3.01	3.07	3.03
$(A_3)_{21}$	0	7.79	1.70	1.40	-41.67	30.84	6.05	2.75	2.69	2.61
$(A_3)_{22}$	9.24	8.23	6.68	9.20	-35.06	14.47	12.64	2.63	2.73	2.83
$(A_4)_{11}$	0.73	0.21	0.70	0.73	3.02	-1.20	0.46	0.23	0.24	0.25
$(A_4)_{12}$	0	0.01	0.07	-0.12	2.24	-0.36	-0.29	-0.23	-0.22	-0.22
$(A_4)_{21}$	0	0.49	-0.03	-0.00	-0.78	1.13	0.15	-0.12	-0.13	-0.14
$(A_4)_{22}$	0.92	1.09	1.01	1.12	0.45	1.21	1.19	0.34	0.33	0.32
Relative Error		0.39	0.17	0.13	2.75	1.38	0.31	0.91	0.91	0.90

Table 2: Numerical results for the inferred 16-dimensional drift coefficient for the two dimensional experiment of Section 3.3. Comparison between the filtering strategies with k_{ma}^1 , $k_{\text{exp}}^{1,1}$, and subsampling. On the first to sixteenth row, the estimated coefficients. On the last row, the relative error.

where, if $X_0^0 \sim \mu^0$, it holds

$$\int_{\mathbb{R}} y \psi^0(y | x, z) dy = \mathbb{E} [X_0^0 | X_\delta^0 = x, Z_\delta^0 = z],$$

i.e., $\psi^0(\cdot | x, z)$ is the conditional density of X_0^0 given $X_\delta^0 = x$ and $Z_\delta^0 = z$.

Proof. In order to prove that the joint process $(X^\varepsilon, Z^\varepsilon)$ is ergodic, we show that it admits a unique invariant measure. If X_0^ε is distributed accordingly to its invariant measure μ^ε , then the processes $(X_s^\varepsilon, 0 \leq s \leq \delta)$ and $(X_s^\varepsilon, t - \delta \leq s \leq t)$ are equally distributed for all $t \geq \delta$. Hence, the two-dimensional random variables $\left(X_\delta^\varepsilon, \frac{1}{\delta} \int_0^\delta X_s^\varepsilon ds\right)$ and $\left(X_t^\varepsilon, \frac{1}{\delta} \int_{t-\delta}^t X_s^\varepsilon ds\right)$ are equal in law for all $t \geq \delta$. Recalling that the joint process $\left(X_t^\varepsilon, \frac{1}{\delta} \int_{t-\delta}^t X_s^\varepsilon ds\right)$ is the solution $(X_t^\varepsilon, Z_t^\varepsilon)$ of the system (4.1), it follows that the invariant measure $\tilde{\mu}^\varepsilon$ on \mathbb{R}^2 is the law of the random variable $\left(X_\delta^\varepsilon, \frac{1}{\delta} \int_0^\delta X_s^\varepsilon ds\right)$. The uniqueness of the invariant measure $\tilde{\mu}^\varepsilon$ is then a direct consequence of the uniqueness of the invariant measure μ^ε for the process X^ε since the joint measure $\tilde{\mu}^\varepsilon$ is uniquely determined by its marginal μ^ε . Moreover, the Fokker–Planck equation for the one-time PDF related to an SDDE with a single fixed delay is well-known (see e.g. [11, 12, 19]) and the stationary equation (4.3) for the density $\tilde{\rho}^\varepsilon$ of $\tilde{\mu}^\varepsilon$ is then obtained due to the particular form of the system (4.1). Finally, the results corresponding to the homogenized system (4.2) can be proved analogously. \square

The following formulas, which will be employed in the proof of the main results, are then direct consequences of the Fokker–Planck equations obtained above.

Lemma 4.2. Let $\tilde{\rho}^\varepsilon(x, z) = \rho^\varepsilon(x)R^\varepsilon(z | x)$, where ρ^ε and $\tilde{\rho}^\varepsilon$ are the densities of the invariant measures μ^ε and $\tilde{\mu}^\varepsilon$ of X^ε and $(X^\varepsilon, Z^\varepsilon)$, respectively, and where R^ε is the conditional density of

Z^ε given X^ε . Then, if $X_0^\varepsilon \sim \mu^\varepsilon$, it holds

$$\sigma \int_{\mathbb{R}} \int_{\mathbb{R}} V'(z) \rho^\varepsilon(x) \partial_x R^\varepsilon(z | x) dx dz = \frac{1}{\delta} \mathbb{E}^{\tilde{\mu}^\varepsilon} [(X_\delta^\varepsilon - Z_\delta^\varepsilon) (X_\delta^\varepsilon - X_0^\varepsilon) V''(Z_\delta^\varepsilon)]. \quad (4.5)$$

Moreover, if δ is independent of ε and writing $\tilde{\rho}^0(x, z) = \rho^0(x) R^0(z | x)$ for the density of the homogenized invariant measure $\tilde{\mu}^0$ of (X^0, Z^0) , it holds

$$\Sigma \int_{\mathbb{R}} \int_{\mathbb{R}} V'(z) \rho^0(x) \partial_x R^0(z | x) dx dz = \frac{1}{\delta} \mathbb{E}^{\tilde{\mu}^0} [(X_\delta^0 - Z_\delta^0) (X_\delta^0 - X_0^0) V''(Z_\delta^0)]. \quad (4.6)$$

Proof. We proceed similarly to the proof of [3, Lemma 3.5]. Replacing the decomposition $\tilde{\rho}^\varepsilon(x, z) = \rho^\varepsilon(x) R^\varepsilon(z | x)$ into the Fokker–Planck equation (4.3) gives

$$\partial_x (\sigma \rho^\varepsilon(x) \partial_x R^\varepsilon(z | x)) + \partial_z \left(\frac{1}{\delta} \left(\int_{\mathbb{R}} y \psi^\varepsilon(y | x, z) dy - x \right) \rho^\varepsilon(x) R^\varepsilon(z | x) \right) = 0.$$

We then multiply the equation above by a smooth function $f: \mathbb{R}^2 \rightarrow \mathbb{R}^N$, $f = f(x, z)$, and integrate first with respect to x and z and then by parts, obtaining

$$\sigma \int_{\mathbb{R}} \int_{\mathbb{R}} \partial_x f(x, z) \rho^\varepsilon(x) \partial_x R^\varepsilon(z | x) dx dz = \frac{1}{\delta} \mathbb{E}^{\tilde{\mu}^\varepsilon} [\partial_z f(X_\delta^\varepsilon, Z_\delta^\varepsilon) (X_\delta^\varepsilon - X_0^\varepsilon)].$$

The choice $f(x, z) = (x - z)V'(z) + V(z)$ gives equation (4.5). Finally, equation (4.6) is obtained analogously employing the Fokker–Planck equation of the homogenized SDE (4.4). \square

4.2 Proof of Main Results

Let us first introduce the notation

$$\begin{aligned} \tilde{\mathcal{M}}_\varepsilon &:= \mathbb{E}^{\tilde{\mu}^\varepsilon} [V'(Z^\varepsilon) \otimes V'(X^\varepsilon)], & \tilde{\mathcal{M}}_0 &:= \mathbb{E}^{\tilde{\mu}^0} [V'(Z^0) \otimes V'(X^0)], \\ \mathcal{M}_\varepsilon &:= \mathbb{E}^{\mu^\varepsilon} [V'(X^\varepsilon) \otimes V'(X^\varepsilon)], & \mathcal{M}_0 &:= \mathbb{E}^{\mu^0} [V'(X^0) \otimes V'(X^0)], \end{aligned}$$

which is repeatedly employed below. Before presenting the main proofs, we introduce two auxiliary lemmas.

Lemma 4.3. *Under Assumption 2.3, it holds*

$$X_\delta^\varepsilon - Z_\delta^\varepsilon = \frac{\sqrt{2\sigma}}{\delta} \int_0^\delta t(1 + \Phi'(Y_t^\varepsilon)) dW_t + R(\varepsilon, \delta), \quad (4.7)$$

where Φ is the solution of the cell problem (1.6) and where the remainder $R(\varepsilon, \delta)$ satisfies for all $p \geq 1$ and a constant $C > 0$ independent of ε and δ

$$\mathbb{E}^{\tilde{\mu}^\varepsilon} [|R(\varepsilon, \delta)|^p]^{1/p} \leq C(\varepsilon + \delta). \quad (4.8)$$

Moreover, if X_0^ε is stationary, i.e. $X_0^\varepsilon \sim \mu^\varepsilon$, it holds

$$\mathbb{E}^{\tilde{\mu}^\varepsilon} [|X^\varepsilon - Z^\varepsilon|^p]^{1/p} \leq C(\delta^{1/2} + \varepsilon), \quad (4.9)$$

$$\mathbb{E}^{\tilde{\mu}^\varepsilon} [|Z^\varepsilon|^p]^{1/p} \leq C. \quad (4.10)$$

Proof. Employing the decomposition (5.8) in [23] and due to [23, Lemma 5.5, Proposition 5.8] we have for all $t \in [0, \delta]$

$$X_\delta^\varepsilon = X_t^\varepsilon + \sqrt{2\sigma} \int_t^\delta (1 + \Phi'(Y_s^\varepsilon)) dW_s + R(\varepsilon, \delta), \quad (4.11)$$

where the remainder satisfies for all $p \geq 1$ and for a constant $C > 0$ independent of ε and δ

$$\mathbb{E}^{\tilde{\mu}^\varepsilon} [|R(\varepsilon, \delta)|^p]^{1/p} \leq C(\varepsilon + \delta).$$

Therefore, we obtain

$$X_\delta^\varepsilon - Z_\delta^\varepsilon = \frac{1}{\delta} \int_0^\delta (X_\delta^\varepsilon - X_t^\varepsilon) dt = \frac{\sqrt{2\sigma}}{\delta} \int_0^\delta \int_t^\delta (1 + \Phi'(Y_s^\varepsilon)) dW_s dt + R(\varepsilon, \delta),$$

which by Fubini's theorem yields

$$X_\delta^\varepsilon - Z_\delta^\varepsilon = \frac{\sqrt{2\sigma}}{\delta} \int_0^\delta t(1 + \Phi'(Y_t^\varepsilon)) dW_t + R(\varepsilon, \delta),$$

and proves (4.7) and (4.8). By the Itô isometry, it holds

$$\mathbb{E}^{\tilde{\mu}^\varepsilon} \left[\left| \int_0^\delta t(1 + \Phi'(Y_t^\varepsilon)) dW_t \right|^p \right]^{1/p} \leq C\delta^{3/2}, \quad (4.12)$$

which, together with (4.7), (4.8) and the proof of Proposition 4.1, gives (4.9). Finally, (4.10) is proved with an application of the triangle inequality and by (4.9) and [23, Corollary 5.4]. \square

Lemma 4.4. *Under Assumption 2.3 and if $\delta = \varepsilon^\zeta$ with $\zeta \in (0, 2)$ then*

$$\lim_{\varepsilon \rightarrow 0} \tilde{\mathcal{M}}_\varepsilon = \mathcal{M}_0.$$

Proof. By the triangle inequality, we have

$$\left\| \tilde{\mathcal{M}}_\varepsilon - \mathcal{M}_0 \right\| \leq \left\| \tilde{\mathcal{M}}_\varepsilon - \mathcal{M}_\varepsilon \right\| + \left\| \mathcal{M}_\varepsilon - \mathcal{M}_0 \right\|.$$

The first term vanishes as $\varepsilon \rightarrow 0$ due to Lemma 4.3, [23, Corollary 5.4] and since V' is Lipschitz under Assumption 2.3. The second term vanishes due to the theory of homogenization as $\varepsilon \rightarrow 0$. \square

We can now prove our main results, i.e., Theorems 2.4 and 2.5.

Proof of Theorem 2.4. Following the proof of [3, Theorem 3.12], we have

$$\widehat{A}(X^\varepsilon, T) = \alpha + I_1 - I_2,$$

where

$$I_1 = \frac{1}{T} M^{-1} \int_0^T \frac{1}{\varepsilon} p' \left(\frac{X_t^\varepsilon}{\varepsilon} \right) V'(Z_t^\varepsilon) dt, \quad I_2 = \frac{\sqrt{2\sigma}}{T} M^{-1} \int_0^T V'(Z_t^\varepsilon) dW_t,$$

and where

$$\lim_{T \rightarrow \infty} I_2 = 0,$$

uniformly in ε by Lemma 4.3 and the strong law of large numbers for martingales. Considering I_1 , the ergodic theorem and an integration by parts yield

$$\lim_{T \rightarrow \infty} I_1 = -\alpha + \tilde{\mathcal{M}}_\varepsilon^{-1} \sigma \int_{\mathbb{R}} \int_{\mathbb{R}} V'(z) \rho^\varepsilon(x) \partial_x R^\varepsilon(z | x) dx dz,$$

where $R^\varepsilon(z | x)$ is defined in Lemma 4.2, which also implies

$$\lim_{T \rightarrow \infty} I_1 = -\alpha + \mathcal{A}^\varepsilon(\delta),$$

where

$$\mathcal{A}^\varepsilon(\delta) = \frac{1}{\delta} \tilde{\mathcal{M}}_\varepsilon^{-1} \mathbb{E}^{\tilde{\mu}^\varepsilon} [(X_\delta^\varepsilon - Z_\delta^\varepsilon)(X_\delta^\varepsilon - X_0^\varepsilon) V''(Z_\delta^\varepsilon)]. \quad (4.13)$$

It remains to show that

$$\lim_{\varepsilon \rightarrow 0} \mathcal{A}^\varepsilon(\delta) = A,$$

for which we consider two cases, corresponding to (2.4) and (2.5), respectively.

Case 1: δ independent of ε . In this case, the theory of homogenization yields

$$\lim_{\varepsilon \rightarrow 0} \mathcal{A}^\varepsilon(\delta) = \frac{1}{\delta} \widetilde{\mathcal{M}}_0^{-1} \mathbb{E}^{\widetilde{\mu}^0} [(X_\delta^0 - Z_\delta^0)(X_\delta^0 - X_0^0)V''(Z_\delta^0)],$$

so that applying Lemma 4.2 for the homogenized equation backwards we have

$$\lim_{\varepsilon \rightarrow 0} \mathcal{A}^\varepsilon(\delta) = \widetilde{\mathcal{M}}_0^{-1} \Sigma \int_{\mathbb{R}} \int_{\mathbb{R}} V'(z) \rho^0(x) \partial_x R^0(z | x) dx dz.$$

An integration by parts then gives

$$\lim_{\varepsilon \rightarrow 0} \mathcal{A}^\varepsilon(\delta) = \widetilde{\mathcal{M}}_0^{-1} \widetilde{\mathcal{M}}_0 A = A,$$

which proves (2.4) and concludes *Case 1*.

Case 2: $\delta = \varepsilon^\zeta$ with $\zeta \in (0, 2)$. Replacing formulas (4.11) with $t = 0$ and (4.7) into (4.13) gives

$$\mathcal{A}^\varepsilon(\delta) = \frac{2\sigma}{\delta^2} \widetilde{\mathcal{M}}_\varepsilon^{-1} \mathbb{E}^{\widetilde{\mu}^\varepsilon} \left[\left(\int_0^\delta t(1 + \Phi'(Y_t^\varepsilon)) dW_t \right) \left(\int_0^\delta (1 + \Phi'(Y_t^\varepsilon)) dW_t \right) V''(Z_\delta^\varepsilon) \right] + \widetilde{R}(\varepsilon, \delta),$$

where, due to Lemma 4.3, estimate (4.12) and the fact that by the Itô isometry

$$\mathbb{E}^{\widetilde{\mu}^\varepsilon} \left[\left| \int_t^\delta (1 + \Phi'(Y_s^\varepsilon)) dW_s \right|^p \right]^{1/p} \leq C \delta^{1/2}, \quad (4.14)$$

it can be shown that the remainder satisfies

$$\left\| \widetilde{R}(\varepsilon, \delta) \right\| \leq C \left(\delta^{1/2} + \varepsilon \delta^{-1/2} + \varepsilon^2 \delta^{-1} \right). \quad (4.15)$$

Moreover, since V'' is Lipschitz under Assumption 2.3 and due to the triangle inequality, equation (4.11), estimates (4.8), (4.14) and Lemma 4.3, it holds for all $t \in [0, \delta]$

$$\mathbb{E}^{\widetilde{\mu}^\varepsilon} [\|V''(Z_\delta^\varepsilon) - V''(X_t^\varepsilon)\|^p]^{1/p} \leq C \left(\varepsilon + \delta^{1/2} \right),$$

which for ε and δ sufficiently small is at most of order $\mathcal{O} \left(\left\| \widetilde{R}(\varepsilon, \delta) \right\| \right)$. Hence, by the Itô isometry

$$\begin{aligned} \mathcal{A}^\varepsilon(\delta) &= \frac{2\sigma}{\delta^2} \widetilde{\mathcal{M}}_\varepsilon^{-1} \mathbb{E}^{\widetilde{\mu}^\varepsilon} \left[\left(\int_0^\delta t(1 + \Phi'(Y_t^\varepsilon)) dW_t \right) \left(\int_0^\delta (1 + \Phi'(Y_t^\varepsilon)) V''(X_t^\varepsilon) dW_t \right) \right] + \widetilde{R}(\varepsilon, \delta) \\ &= \frac{2\sigma}{\delta^2} \widetilde{\mathcal{M}}_\varepsilon^{-1} \int_0^\delta t \mathbb{E}^{\widetilde{\mu}^\varepsilon} [(1 + \Phi'(Y_t^\varepsilon))^2 V''(X_t^\varepsilon)] dt + \widetilde{R}(\varepsilon, \delta). \end{aligned}$$

Repeating the last part of the proof of [3, Lemma 3.17], we then obtain

$$\begin{aligned} \mathcal{A}^\varepsilon(\delta) &= \frac{2\sigma\mathcal{K}}{\delta^2} \widetilde{\mathcal{M}}_\varepsilon^{-1} \mathbb{E}^{\mu^0} [V''(X^0)] \int_0^\delta t dt + \widetilde{R}(\varepsilon, \delta) \\ &= \Sigma \widetilde{\mathcal{M}}_\varepsilon^{-1} \mathbb{E}^{\mu^0} [V''(X^0)] + \widetilde{R}(\varepsilon, \delta). \end{aligned}$$

Finally, since $\delta = \varepsilon^\zeta$ with $\zeta \in (0, 2)$, by (4.15) and due to Lemma 4.4 we obtain

$$\lim_{\varepsilon \rightarrow 0} \mathcal{A}^\varepsilon(\delta) = \Sigma \mathcal{M}_0^{-1} \mathbb{E}^{\mu^0} [V''(X^0)],$$

and an integration by parts gives

$$\lim_{\varepsilon \rightarrow 0} \mathcal{A}^\varepsilon(\delta) = \Sigma \mathcal{M}_0^{-1} \frac{1}{\Sigma} \mathcal{M}_0 A = A,$$

which proves (2.5) and therefore concludes the proof. \square

Proof of Theorem 2.5. The ergodic theorem gives

$$\lim_{T \rightarrow \infty} \widehat{\Sigma}(X^\varepsilon, T) = \frac{1}{\delta} \mathbb{E}^{\widetilde{\mu}^\varepsilon} [(X_\delta^\varepsilon - Z_\delta^\varepsilon)(X_\delta^\varepsilon - X_0^\varepsilon)].$$

Following step-by-step *Case 2* of the proof of Theorem 2.4 with the value 1 instead of $V''(Z_\delta^\varepsilon)$, and without the pre-multiplication by $\widetilde{\mathcal{M}}_\varepsilon^{-1}$, we obtain the desired result. \square

5 Conclusion

In this work, we introduced a novel methodology for inferring effective diffusions from observations of multiscale dynamics based on filtering the data with moving averages. The method, which is an improvement of our previous work [3], is robust, easy to implement, and outperforms the standard technique of subsampling on a range of test cases. Theoretical justification is provided by rigorous results of unbiasedness in the asymptotic limit of $T \rightarrow \infty$ and $\varepsilon \rightarrow 0$. We notice here that this paper answers to point (i) in the conclusion of [3]. Indeed, we analysed here the limit of the exponential filtering approach, explored in that work, for $\beta \rightarrow \infty$. The analysis for finite values of $\beta > 1$ is still unresolved, but due to the fast stabilization of the exponential filter with respect to β , we believe this work provides a satisfactory answer.

Acknowledgements

The authors are partially supported by the Swiss National Science Foundation, under grant No. 200020_172710.

References

- [1] A. ABDULLE AND A. DI BLASIO, *Numerical homogenization and model order reduction for multiscale inverse problems*, Multiscale Model. Simul., 17 (2019), pp. 399–433.
- [2] A. ABDULLE AND A. DI BLASIO, *A Bayesian Numerical Homogenization Method for Elliptic Multiscale Inverse Problems*, SIAM/ASA J. Uncertain. Quantif., 8 (2020), pp. 414–450.
- [3] A. ABDULLE, G. GAREGNANI, G. A. PAVLIOTIS, A. M. STUART, AND A. ZANONI, *Drift estimation of multiscale diffusions based on filtered data*. to appear in Found. Comput. Math., 2021.
- [4] A. ABDULLE, G. GAREGNANI, AND A. ZANONI, *Ensemble Kalman Filter for Multiscale Inverse Problems*, Multiscale Model. Simul., 18 (2020), pp. 1565–1594.
- [5] A. ABDULLE, G. A. PAVLIOTIS, AND A. ZANONI, *Eigenfunction martingale estimating functions and filtered data for drift estimation of discretely observed multiscale diffusions*. arXiv preprint arXiv:2104.10587, 2021.
- [6] Y. AÏT-SAHALIA AND J. JACOD, *High-frequency financial econometrics*, Princeton University Press, 2014.
- [7] A. BENSOUSSAN, J.-L. LIONS, AND G. PAPANICOLAOU, *Asymptotic analysis for periodic structures*, North-Holland Publishing Co., Amsterdam, 1978.
- [8] C. J. COTTER AND G. A. PAVLIOTIS, *Estimating eddy diffusivities from noisy Lagrangian observations*, Commun. Math. Sci., 7 (2009), pp. 805–838.
- [9] D. CROMMELIN AND E. VANDEN-EIJNDEN, *Reconstruction of diffusions using spectral data from timeseries*, Commun. Math. Sci., 4 (2006), pp. 651–668.

- [10] D. CROMMELIN AND E. VANDEN-EIJNDEN, *Diffusion estimation from multiscale data by operator eigenpairs*, Multiscale Model. Simul., 9 (2011), pp. 1588–1623.
- [11] T. D. FRANK, *Delay Fokker–Planck equations, Novikov’s theorem, and Boltzmann distributions as small delay approximations*, Phys. Rev. E, 72 (2005), p. 011112.
- [12] S. GUILLOUZIC, I. L’HEUREUX, AND A. LONGTIN, *Small delay approximation of stochastic delay differential equations*, Phys. Rev. E, 59 (1999), pp. 3970–3982.
- [13] S. KALLIADASIS, S. KRUMSCHEID, AND G. A. PAVLIOTIS, *A new framework for extracting coarse-grained models from time series with multiscale structure*, J. Comput. Phys., 296 (2015), pp. 314–328.
- [14] S. KRUMSCHEID, G. A. PAVLIOTIS, AND S. KALLIADASIS, *Semiparametric drift and diffusion estimation for multiscale diffusions*, Multiscale Model. Simul., 11 (2013), pp. 442–473.
- [15] S. KRUMSCHEID, M. PRADAS, G. A. PAVLIOTIS, AND S. KALLIADASIS, *Data-driven coarse graining in action: Modeling and prediction of complex systems*, Physical Review E, 92 (2015), p. 042139.
- [16] T. LELIÈVRE AND G. STOLTZ, *Partial differential equations and stochastic methods in molecular dynamics*, Acta Numer., 25 (2016), pp. 681–880.
- [17] R. S. LIPTSER AND A. N. SHIRYAEV, *Statistics of random processes. I*, vol. 5 of Applications of Mathematics (New York), Springer-Verlag, Berlin, expanded ed., 2001. General theory, Translated from the 1974 Russian original by A. B. Aries, Stochastic Modelling and Applied Probability.
- [18] R. S. LIPTSER AND A. N. SHIRYAEV, *Statistics of random processes. II*, vol. 6 of Applications of Mathematics (New York), Springer-Verlag, Berlin, expanded ed., 2001. Applications, Translated from the 1974 Russian original by A. B. Aries, Stochastic Modelling and Applied Probability.
- [19] S. A. M. LOOS AND S. H. L. KLAPP, *Fokker–Planck equations for time-delayed systems via Markovian embedding*, J. Stat. Phys., 177 (2019), pp. 95–118.
- [20] J. NOLEN, G. A. PAVLIOTIS, AND A. M. STUART, *Multiscale modeling and inverse problems*, in Numerical analysis of multiscale problems, vol. 83 of Lect. Notes Comput. Sci. Eng., Springer, Heidelberg, 2012, pp. 1–34.
- [21] G. A. PAVLIOTIS, *Stochastic processes and applications*, vol. 60 of Texts in Applied Mathematics, Springer, New York, 2014. Diffusion processes, the Fokker-Planck and Langevin equations.
- [22] G. A. PAVLIOTIS, Y. POKERN, AND A. M. STUART, *Parameter estimation for multiscale diffusions: an overview*, in Statistical methods for stochastic differential equations, vol. 124 of Monogr. Statist. Appl. Probab., CRC Press, Boca Raton, FL, 2012, pp. 429–472.
- [23] G. A. PAVLIOTIS AND A. M. STUART, *Parameter estimation for multiscale diffusions*, J. Stat. Phys., 127 (2007), pp. 741–781.
- [24] G. A. PAVLIOTIS AND A. M. STUART, *Multiscale methods: averaging and homogenization*, vol. 53 of Texts in Applied Mathematics, Springer, New York, 2008.
- [25] Y. POKERN, A. M. STUART, AND E. VANDEN-EIJNDEN, *Remarks on drift estimation for diffusion processes*, Multiscale Model. Simul., 8 (2009), pp. 69–95.
- [26] L. ZHANG, P. A. MYKLAND, AND Y. AÏT-SAHALIA, *A tale of two time scales: determining integrated volatility with noisy high-frequency data*, J. Amer. Statist. Assoc., 100 (2005), pp. 1394–1411.